

## Theory of Two-Photon Polarization Spectroscopy of Plasma-Broadened Hydrogen $L_\alpha$ Line

Joachim Seidel

*Physikalisch-Technische Bundesanstalt, Institut Berlin, D-1000 Berlin 10, West Germany*

(Received 11 June 1986)

The Stark-broadened line profile observed with Doppler-free two-photon polarization spectroscopy of the hydrogen resonance line  $L_\alpha$  in a plasma is investigated theoretically. With use of computer simulations for the numerical evaluation of line profiles, strong ion dynamical effects in the line core are found at moderate plasma densities.

PACS numbers: 32.70.Jz, 32.60.+i

With conventional emission or absorption spectroscopy, Stark broadening of hydrogen lines in plasmas cannot be measured at low electron densities because it is hidden by Doppler broadening. For the Lyman line  $L_\alpha$ , the preferential test object of theory since its first successful measurement,<sup>1</sup> the Stark width is larger than the Doppler width only at  $N_e \geq 10^{23} \text{ m}^{-3}$ , for temperatures of about  $10^4 \text{ K}$ . Yet, experimental determination of  $L_\alpha$  Stark broadening at lower electron densities would be highly desirable, considering, e.g., that new theoretical approaches<sup>2,3</sup> predict ion dynamical effects to increase the  $L_\alpha$  Stark width at  $N_e \approx 10^{21} \text{ m}^{-3}$  by an order of magnitude. The experimental determination of hydrogen Stark broadening in this range of plasma densities has now become possible, as the first Doppler-free measurement of a Stark-broadened line profile from a dense plasma has recently been accomplished with  $L_\alpha$  two-photon resonant polarization spectroscopy,<sup>4</sup> providing the first example of Doppler-free two-photon polarization spectroscopy at all. The present Letter is intended to supply theoretical data for this new kind of plasma spectroscopy.

The basic principle of the method is easily understood<sup>5</sup>: Consider a homogeneous layer of isotropic plasma between  $z=0$  and  $z=d$ , a probe wave with electric field  $\text{Re}F_1(z) \exp(ik_1z - i\Omega_1t)$  propagating along the  $z$  axis, and a counterpropagating pump wave  $\text{Re}F_2(z) \exp(-ik_2z - i\Omega_2t)$ , the probe wave being linearly polarized before it enters the plasma,  $F_1(z \leq 0) = F_{10} = F_{10}\mathbf{e}_x$ , and the pump wave circularly polarized,  $F_2(z \geq d) = F_{20} = F_{20}\mathbf{e}_-$ , with  $\mathbf{e}_- = (\mathbf{e}_x - i\mathbf{e}_y)/\sqrt{2}$ . The pump wave induces an optical anisotropy in the plasma, by which the probe wave becomes elliptically polarized, leaving the plasma with amplitude  $F_1(z \geq d) = F_{10} + \delta F_1$ . A cross-polarization analyzer blocking  $F_{10}$  separates the  $y$  component of  $\delta F_1$ , and the corresponding irradiance  $E$  is measured as a function of frequency. In the experiment,  $\Omega_1 = \Omega_2 \approx \omega_{21}/2$ , half the  $L_\alpha$  frequency, to eliminate Doppler broadening. For the theoretical discussion, I take  $\Omega_1$  and  $\Omega_2$  as independent at first, with  $\Omega_1 \approx \Omega_2 \approx \omega_{21}/2$ . On the assumption that the two-photon  $L_\alpha$  resonance is the only resonance in the plas-

ma to affect the waves, the dielectric tensor for the probe wave inside the plasma is  $\epsilon(\Omega_1) = \epsilon_0[1 + \chi(\Omega_1; \Omega_2)]$ , the susceptibility being due to the pump wave. Its imaginary part describes the induced dichroism and its real part the associated birefringence (optical Kerr effect), for radiation at the probe frequency. Strictly, one should also account for a self-induced contribution  $\chi(\Omega_1; \Omega_1)$  as well as corresponding effects on the pump wave, which would lead to nonlinear coupling of probe- and pump-wave propagation in the plasma.<sup>6</sup> However, for the hydrogen  $L_\alpha$  transition, the total effect on the amplitudes is small in all practical cases, since there is no enhancement by resonance with an intermediate level. In addition, the pump wave will usually be stronger than the probe wave. Under these conditions, one can (i) neglect the probe-wave contribution to  $\epsilon(\Omega_1)$ , and (ii) calculate  $\chi(\Omega_1; \Omega_2)$  with  $F_{20}$  instead of  $F_2(z)$ , without introducing noticeable errors in  $\delta F_1$ . This makes  $\epsilon(\Omega_1)$  constant along  $z$ . For any isotropic medium,  $\chi(\Omega_1; \Omega_2)$  can be expressed<sup>6</sup> in terms of the three independent components  $\chi_{xxyy}^{(3)}$ ,  $\chi_{xyxy}^{(3)}$ , and  $\chi_{xyyx}^{(3)}$  of the two-photon resonant part of the third-order nonlinear susceptibility tensor  $\chi^{(3)}(\Omega_1, \Omega_2, -\Omega_2)$ . For the two-photon  $s$ - $s$   $L_\alpha$  transition (the upper level  $n=2$  contains no  $d$  state), the selection rules<sup>7</sup> forbid interaction of orthogonally polarized waves,  $\mathbf{F}_1 \cdot \mathbf{F}_2 = 0$ . Accordingly,  $\chi_{xxyy}^{(3)}$  and  $\chi_{xyxy}^{(3)}$  vanish in this case, and we have, denoting  $\chi_{xyyx}^{(3)}(\Omega_1, \Omega_2, -\Omega_2)$  by  $\chi^{(3)}(\Omega_1, \Omega_2)$ ,

$$\chi(\Omega_1; \Omega_2) = \chi^{(3)}(\Omega_1, \Omega_2) |F_{20}|^2 \mathbf{e}_- \mathbf{e}_- \quad (1)$$

for the circularly polarized pump wave considered here. The eigenvectors of  $\chi$  being  $\mathbf{e}_-$  and  $\mathbf{e}_+ = -\mathbf{e}_-$ , with eigenvalues 0 and  $\chi^{(3)}(\Omega_1, \Omega_2) |F_{20}|^2$ , respectively, it is easy to calculate the irradiance  $E = \epsilon_0 c_0 \times |\delta F_{1y}|^2/2$  produced by  $\delta F_{1y}$  behind the analyzer:

$$E = \frac{1}{4} (\Omega_1^2 d^2 / \epsilon_0^2 c_0^4) |\chi^{(3)}(\Omega_1, \Omega_2)|^2 E_{20}^2 E_{10}, \quad (2)$$

where pump and probe irradiances have been introduced as well.

For evaluation of  $\chi^{(3)}(\Omega_1, \Omega_2)$ , which varies strongly near the two-photon resonance and deter-

mines the observed line profile, we cannot refer to standard results<sup>6</sup> describing line broadening by relaxation times, i.e., Lorentz profiles, which are not appropriate for hydrogen Stark broadening in plasmas. However, we can use results<sup>7</sup> for the atomic  $n=1 \rightarrow n=2$  two-photon transition rate  $W_2$  in a plasma to express  $\text{Im}\chi^{(3)}$ , and a Kramers-Kronig relation to calculate  $\text{Re}\chi^{(3)}$ .

$W_2$  was evaluated<sup>7</sup> under approximations well proved for plasma-broadened one-photon emission line profiles. An evolution operator  $T(t)$  describes the effect of the plasma on the degenerate atomic states of level  $n=2$ , according to the Schrödinger equation  $i\hbar \dot{T} = -\mathbf{d} \cdot \mathbf{F}(t) T$ , with  $\mathbf{d}$  the atomic dipole moment and  $\mathbf{F}(t)$  the electric plasma microfield acting on the atom (dipole-interaction approximation). With  $\langle 2s|T(t)|2s \rangle$  denoted by  $C(t)$ , the frequency dependence of  $W_2$  is determined by

$$\tilde{R}(\Delta\omega) = \text{Re}\tilde{C}(\Delta\omega) = \text{Re} \int_0^\infty dt \exp(i\Delta\omega t) C(t),$$

where  $\Delta\omega = \Omega_1 + \Omega_2 - \omega_{21} - (\mathbf{k}_1 + \mathbf{k}_2) \cdot \mathbf{v}$  is the frequency distance from exact resonance, Doppler shifts included:

$$W_2 = 2(\hbar\epsilon_0 c_0)^{-2} E_1 E_2 |\langle 1s|\alpha|2s \rangle|^2 \{\tilde{R}(\Delta\omega)\}. \quad (3)$$

Braces indicate an average over all  $\mathbf{F}(t)$  and atomic velocities  $\mathbf{v}$ . Atomic velocities can be taken as constant in time here because velocity-changing collisions (VCC) on (neutral) hydrogen atoms act too slowly even in dense plasmas to affect  $W_2$ . With a hard-sphere model, velocity relaxation times are estimated<sup>8</sup> to be of the order of 1 ns ( $N_e = 10^{23} \text{ m}^{-3}$ ) to 100 ns ( $N_e = 10^{21} \text{ m}^{-3}$ ). In the hydrogen  $L_\alpha$  two-photon transition, with no intermediate atomic energy level, absorption of the first photon leaves the atom in a state which lives for only about 1 fs. Within this time, absorption of the second photon has to set in. On the VCC time scale, therefore, absorption starts simultaneously for both photons, and the "Doppler phases" due to atomic motion along  $\mathbf{r}(t)$ , which appear in the evaluation of  $W_2$ , become  $\mathbf{k}_j \cdot [\mathbf{r}(t) - \mathbf{r}(0)]$ ,  $j=1,2$ . In the Doppler-free case,  $\mathbf{k}_2 = -\mathbf{k}_1$ , they always cancel, regardless of VCC, even if absorption goes into a narrow line profile  $\{\tilde{R}(\Delta\omega)\}$  and takes long to complete because of the corresponding slow decay of  $\{C(t)\}$  from its initial value of 1. Actually, in a plasma, Stark broadening makes  $\{C(t)\}$  decay rapidly as compared to VCC times: From the half-widths<sup>7</sup> of  $\{\tilde{R}(\Delta\omega)\}$ , decay times of about 0.3 ps ( $N_e = 10^{23} \text{ m}^{-3}$ ) to 5 ps ( $N_e = 10^{21} \text{ m}^{-3}$ , cf. Fig. 1) are found for  $\{C(t)\}$ . Thus, VCC can be neglected in any case, Doppler-free or not, and need not be considered in the calculation of the Stark profiles either.

Equation (3) gives the mean atomic  $L_\alpha$  transition rate due to absorption of two photons, one from each of the two modes of the electromagnetic field, which

corresponds to  $\chi^{(3)}(\Omega_1, \Omega_2, -\Omega_2)$ . While two-photon absorption is described by  $\langle 2s|T|2s \rangle$ , one-photon line profiles are obtained from the diagonal  $2p$  matrix elements of  $T$ . Thus, one- and two-photon line profiles are closely connected. As to their general form, however, two-photon  $L_\alpha$  Stark profiles differ from one-photon  $L_\alpha$  profiles and rather resemble one-photon  $L_\beta$  profiles, because  $|2s \rangle$  is a linear combination of shifted Stark states (energy-level shifts  $\pm 3ea_0 F$  in a static electric field  $F$ ), without a contribution from unshifted states.

The quantity  $\alpha$  giving the "line strength" in Eq. (3) is a "hyperpolarizability."<sup>6</sup> Strictly,  $\langle 1s|\alpha|2s \rangle$  varies with  $\Omega_1$  and  $\Omega_2$ , but this variation is very weak for  $\Omega_1 \approx \Omega_2 \approx \omega_{21}/2$  and can be neglected over the line profile, with  $\Omega_1$  and  $\Omega_2$  replaced by  $\omega_{21}/2$  when calculating the matrix element<sup>7</sup>:

$$\langle 1s|\alpha|2s \rangle = -7.854 \times 4\pi\epsilon_0 a_0^3 \mathbf{e}_1 \cdot \mathbf{e}_2, \quad (4)$$

with  $a_0 \approx 53$  pm the Bohr radius. As to the polarization dependence, here we recover the selection rule which was used to obtain Eq. (1).

The connection of  $W_2$  and  $\text{Im}\chi^{(3)}(\Omega_1, \Omega_2)$  is established by consideration of the probe-wave absorption in a thin layer of plasma containing ground-state hydrogen atoms with density  $N_1$ . Provided that the population of the upper level  $n=2$  is negligible, no correction is needed for stimulated emission, and we obtain

$$\text{Im}\chi^{(3)}(\Omega_1, \Omega_2) = (4\pi \times 7.854)^2 \epsilon_0 a_0^6 \hbar^{-1} N_1 \{\tilde{R}(\Delta\omega)\}. \quad (5)$$

Equation (5) shows that  $\text{Im}\chi^{(3)}(\Omega_1, \Omega_2)$  depends on  $\Omega_1, \Omega_2$  only through  $\Delta\omega$ , the argument of  $\tilde{R}$ . The Kramers-Kronig relation which is known to hold with respect to  $\Omega_1$  (at fixed  $\Omega_2$ ), for reasons of causality,<sup>6</sup> can then be rewritten as a Kramers-Kronig relation with respect to  $\Delta\omega$ . This shows that  $\chi^{(3)}(\Omega_1, \Omega_2)$  is given by the right-hand side of Eq. (5) with  $\tilde{R}$  replaced by  $i\tilde{C}$ :

$$\chi^{(3)}(\Omega_1, \Omega_2) = i(4\pi \times 7.854)^2 \epsilon_0 a_0^6 \hbar^{-1} N_1 \{\tilde{C}(\Delta\omega)\}. \quad (6)$$

Especially for the Doppler-free case with  $\Omega_1 = \Omega_2 = \Omega$ ,  $\mathbf{k}_2 = -\mathbf{k}_1$ , the Fourier transform  $\tilde{C}$  is taken at  $\Delta\omega = 2\Delta\Omega = 2\Omega - \omega_{21}$ . At last, we examine the line profile  $\{|\tilde{C}(\Delta\omega)|\}^2$ , noting that  $C(t)$  is real under the dipole-interaction approximation. Accordingly, the real and imaginary parts of  $\{\tilde{C}(\Delta\omega)\}$  are proportional to the cosine and sine transforms of  $\{C(t)\}$ , and the sum of their squares can be written as the cosine transform of an autocorrelation function of  $\{C\}$ :

$$\begin{aligned} & \{|\tilde{C}(\Delta\omega)|\}^2 \\ &= 2 \int_0^\infty dt \cos(\Delta\omega t) \int_0^\infty ds \{C(s)\} \{C(s+t)\}. \quad (7) \end{aligned}$$

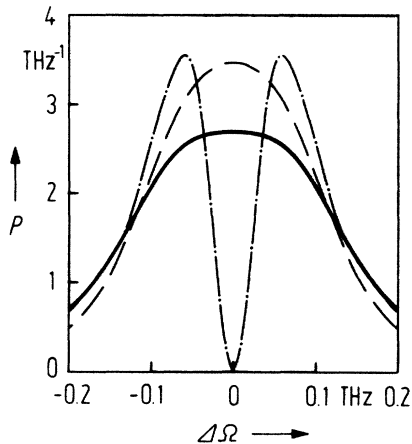


FIG. 1. Area-normalized Doppler-free two-photon profiles of hydrogen  $L_\alpha$  line Stark broadened in an  $\text{Ar}^+$  plasma with electron density  $10^{21} \text{ m}^{-3}$  and temperature  $10^4 \text{ K}$ . Solid line, polarization profile; dashed line, absorption profile (both with ion dynamical effects included); dot-dashed line, polarization profile for "static ions" (ion dynamical effects neglected).  $\Delta\Omega$  is the (laser) frequency separation from half the one-photon  $L_\alpha$  frequency,  $\omega_{21}/2$ , which corresponds to a wavelength of about 243 nm.

It is only in special cases that the line profile measured by polarization spectroscopy has the same shape as the absorption line profile, proportional to the cosine transform of  $\{C(t)\}$ , e.g., for Lorentz profiles with  $\{C(t)\} = \exp(-t/\tau)$ , the one case usually discussed in the literature. Equation (7) shows that polarization and absorption profiles are different in general. An easy-to-calculate example<sup>9</sup> is provided by the superposition of two symmetrically shifted Lorentz profiles (cf. Fig. 1 as well).

Having completed the formal derivation of the frequency dependence of the irradiance  $E$  observed in experiment, we are left with the calculation of  $\{T(t)\}$  or its Fourier transform. This is a difficult problem on its own, but has been discussed in detail in connection with the plasma broadening of the one-photon  $L_\alpha$  profile.<sup>10</sup> At present, the most reliable theoretical method to calculate line profiles is computer simulation of the broadening by plasma ions,<sup>11,12</sup> with employment of an analytical expression for the effects of electron-impact broadening. Simulations for the one-photon  $L_\alpha$  profile are easily modified to yield results for two-photon  $L_\alpha$  absorption and polarization profiles. In Fig. 1 are shown examples of area-normalized profiles for

an electron density of  $10^{21} \text{ m}^{-3}$  and a plasma temperature of  $10^4 \text{ K}$ , for  $\text{Ar}^+$  plasma ions. The ions were treated as immovable in the computations, but the Maxwell distribution of absorber (H atoms) velocities was correctly taken into account<sup>11,12</sup>. The ion dynamical effects (due to atomic motion in this case) are seen to alter the line center completely as compared to the "static ions" profile involving neglect of relative atom-ion motion. The difference between polarization and absorption profiles (both with ion dynamical effects included) is also apparent in Fig. 1. Similar results have been obtained for an electron density of  $10^{22} \text{ m}^{-3}$ .

In Ref. 4, the theoretical polarization profile for an electron density of  $5 \times 10^{22} \text{ m}^{-3}$  is compared with the first measured profile of this kind. The profiles are found to agree well, an indication that reliable line profiles can be computed from the theoretical expressions derived above, Eqs. (2), (6), and (7), if due account is taken of ion dynamical effects, e.g., by use of a computer simulation.

<sup>1</sup>K. Grützmacher and B. Wende, Phys. Rev. A 16, 243 (1977).

<sup>2</sup>J. Seidel, Z. Naturforsch. 32a, 1207 (1977).

<sup>3</sup>R. Stamm, E. W. Smith, and B. Talin, Phys. Rev. A 30, 2039 (1984).

<sup>4</sup>K. Danzmann, K. Grützmacher, and B. Wende, preceding Letter [Phys. Rev. Lett. 57, 2151 (1986)].

<sup>5</sup>P. F. Liao and G. C. Bjorklund, Phys. Rev. Lett. 36, 584 (1976).

<sup>6</sup>M. Schubert and B. Wilhelmi, in *Einführung in die Nichtlineare Optik, Teil I* (Teubner, Leipzig, 1971), and in *Einführung in die Nichtlineare Optik, Teil II* (Teubner, Leipzig, 1978). See also Y. R. Shen, in *The Principles of Nonlinear Optics* (Wiley, New York, 1984).

<sup>7</sup>J. Seidel, in *Spectral Line Shapes*, edited by K. Burnett (De Gruyter, Berlin, 1983), Vol. 2, p. 381. In this reference, a factor of  $(4\pi\epsilon_0)^{-4}$  is missing in the definition of the two-photon transition operator and should be supplemented in the right-hand side of the equation following Eq. (6) on p. 385.

<sup>8</sup>D. D. Burgess, in *Spectral Line Shapes*, edited by B. Wende (De Gruyter, Berlin, 1981), p. 473.

<sup>9</sup>K. Danzmann, private communication.

<sup>10</sup>J. Seidel, in *Spectral Line Shapes*, edited B. Wende (De Gruyter, Berlin, 1981), p. 3.

<sup>11</sup>J. Seidel and R. Stamm, J. Quant. Spectrosc. Radiat. Transfer 27, 499 (1982).

<sup>12</sup>J. Seidel, in *Spectral Line Shapes*, edited by F. Rostas (De Gruyter, Berlin, 1985), Vol. 3, p. 69.